

The Utility of Digital Imaging Technologies for the Virtual Curation and
Metric Analysis of Skeletal Remains

By
Devin Adcox

A thesis presented to the Honors College of Middle Tennessee State University in partial
fulfillment of the requirements for graduation from the University Honors College

Fall 2019

The Utility of Digital Imaging Technologies for the Virtual Curation and Metric
Analysis of Skeletal Remains

by
Devin Adcox

APPROVED:

Dr. Tiffany Saul
Anthropology Department

Dr. Brandon Wallace
Sociology/Anthropology
Department

Dr. Philip E. Phillips, Associate
Dean University Honors College

Dedicated to my parents as well as my advisors and friends. I never could have accomplished this without everyone's help and support.

Acknowledgements

First, I would like to acknowledge the anatomical comparatives. They are individuals regardless of whether they are cast and they should be treated with respect and dignity. Second, I would like to acknowledge the Forensic Institute for Research and Education for providing access to lab space, and equipment.

Abstract

New artifact curation methods such as 3-D laser scanning and 3-D photogrammetry are exciting new developments within the field of anthropology. However, there is little research discussing the accuracy and comparability of these measurements to more traditional methods of curation such as hand held metrics. This research compares the accuracies and comparability of 3-D laser scanning, 3-D photogrammetry, and a Microscribe digitizer to traditional hand held metrics. 3-D models were generated for three different skulls using a NextEngine laser scanner and photogrammetry. Cranial metrics were repeated nine times for each digitally created model produced via the NextEngine Laser Scanner or 3-D Photogrammetry and nine times on the physical skull using a Microscribe digitizer and hand held calipers. Analyses of these measurements revealed that the technological platforms are comparable in accuracy supporting the use of these technologies as a digital curation method.

Table of Contents

Signature Page.....	ii
Dedication Page.....	iii
Aknowledgements.....	iv
Abstract.....	v
List of Tables	vii
List of Figures.....	viii
I. Introduction.....	1
A. 3-D Laser Scanning	
B. 3-D Photogrammetry	
C. Microscribe 3-D digitizer	
II. Material and Methods.....	5
A. Hand Held Metrics	
B. 3-D Laser Scanning	
C. 3-D Photogrammetry	
D. Microscribe 3-D digitizer	
III. Results.....	20
IV. Discussion.....	27
V. Conclusion.....	31
VI. Works Cited	33
VII. Appendix.....	38

List of Tables

Table 1: Description of each skull used in the analysis of craniometrics.	6
Table 2: Comparison of the Microscribe 3-D Digitizer to hand-held metrics for each dataset.....	21
Table 3: Comparison of the NextEngine 3-D Laser Scanner to hand-held metrics for each data set.....	22
Table 4: Comparison of 3-D photogrammetry to hand-held metrics for each data set.	22
Table 5: Comparison of Measurement data sets for Hand Held metrics	23
Table 6: Comparison of Measurements between data sets for Measurements taken on Photogrammetry Models	23
Table 7: Comparison of Measurements between data sets for Measurements taken on Models produced by the NextEngine Laser Scanner.....	24
Table 8: Comparison of Measurements between data sets for the Microscribe 3-D Digitizer.....	24
Table 9: Comparison of the ranges of the measurements taken with the Microscribe 3-D digitizer to the ranges of measurements taken with Hand Held Instruments.....	26
Table 10: Comparison of the ranges of measurements taken on Models made with the 3-D laser scanner to the ranges of measurements taken on Hand Held Instruments...	27
Table 11: Comparison of the ranges of measurements taken on Models made with the 3-D Photogrammetry to the ranges of measurements taken on Hand Held Instruments.....	27

List of Figures

Figure 1: Photograph of the anterior view of Individual 2 Cast	7
Figure 2: Photograph of the superior view of Individual 2 cast's skull illustrating the degree of cranial suture fusion.	7
Figure 3: Photograph of the anterior view of Individual 3 note the slight taphonomic damage to the maxilla, superior to the central incisors.....	8
Figure 4: Photograph of the superior view of Individual 3's Skull Illustrating the Degree of cranial suture closure.	8
Figure 5: Photograph of the anterior view of Individual 1	9
Figure 6: Photograph of the superior view of Individual 1's skull illustrating the degree of cranial suture closure.	9
Figure 7: Diagram illustrating a subset of the cranial landmark measurements taken, from Data Collection Procedures for Forensic Skeletal Material (13).	10
Figure 8: Set-up used for the NextEngine 3-D Laser Scanner.	11
Figure 9: 3-D Model of Individual 2 generated by the NextEngine Laser Scanner illustrating a subset of measurement points placed in Meshlab.....	12
Figure 10: 3-D Model of Individual 2 created by the NextEngine Laser Scanner placed in Meshlab.	13
Figure 11: 3-D Model of Individual 1 created by the NextEngine 3-D Laser Scanner placed in Meshlab.....	13
Figure 12: Model of Individual 3 created using the NextEngine 3-D Laser Scanner placed in Meshlab.	14

Figure 13: Photogrammetry set up with Individual 2 placed on the rotating turn table. Softbox lights are set up above and to the right and left of the subject. Can lights are set in front of the subject beside the camera.	15
Figure 14: Position of camera relative to subject during shooting.	16
Figure 15: 3-D model of Individual 2 (cast) produced by photogrammetry with a subset of measurements placed across the skull.	17
Figure 16: 3-D model of Individual 2 (cast) created via photogrammetry.	18
Figure 17: 3-D model of Individual 1 created via photogrammetry.	18
Figure 18: 3-D model of Individual 3 created via photogrammetry.	19
Figure 19: Typical set up of the Microscribe 3-D Digitizer.	20
Figure 20: ANOVA graph illustrating the relatedness of different variables. In this case it is illustrating datasets.	25
Figure 21: ANOVA graph illustrating the relationship of the Individual skull to the measurements.	25
Figure 22: ANOVA graph illustrating the relationship of the technological platform to the measurements produced.	25

Introduction

The curation and documentation of skeletal remains has been a driving force behind biological anthropology since its inception. Standard methods include photography, detailed notes, and manually-derived measurements of the remains according to guidelines established in publications such as *Data Collection Procedures for Forensic Skeletal Material 2.0* (13). Today there are additional avenues of curation available to anthropologists through technologies such as the MicroScribe 3-D Digitizer and techniques such as 3-D photogrammetry. The advantage behind these techniques is that, unlike photographs, they create a three-dimensional model that can be rotated, measured, and shared with other researchers. The creation of measurable models that can be shared among researchers allows for greater access to osteological collections making research easier to accomplish. An easier route of 3-D imaging for anthropologists to take is 3-D laser scanning. It is more intuitive since images are automatically generated by the program, and the researcher can see what regions need to be scanned.

3-D Laser Scanning

3-D Laser scanning involves the creation of a digital model using lasers to map the surface of an object. Within archaeology and anthropology today, 3-D laser scanning is being used to curate lithic artifacts, pottery, sculptures, and early hominin fossils (3, 6, 8, 10, 14, 21, 25). Additionally, there are entire websites dedicated to curating examples of trauma and pathology (26). These projects illustrate the ability that 3-D curation has in providing anthropological data to researchers and the anthropology community.

Currently, there is very little research that compares the accuracy of 3-D laser scanning to other technological platforms with the exception of the work done by Erickson et. al. (7) and the work of Algee-Hewitt and Wheat (2). Algee-Hewitt and

Wheat's research compared the coordinate data of measurement points placed in Meshlab, an open source program that allows for the optimization of three dimensional models, to the coordinate data of the same points placed using the Microscribe 3-D digitizer (2, 5). In addition to this, they compared the quality of a subset of inter-landmark measurements by repeating the same measurements multiple times across all of the platforms (2). The goals behind this research project and Algee-Hewitt and Wheat's research are similar since both seek to answer the question of reliability and accuracy of different technological platforms.

However, this project differs from that of Algee-Hewitt and Wheat whose project divided the measurement landmarks into three different types based on previous research that quantified the points based on how they are measured. The current analysis only compares the quality of inter-landmark measurements (2). This research also features a more exhaustive list of measurements, examining all 27 cranial measurements commonly used in anthropological analyses of human crania. This analysis was designed to determine whether any measurements produced significant variation within a technological platform. Additionally, this project provides greater information about inter-landmark measurements taken across the skull since it seeks to generate information about all of the measurements across the skull rather than just a subset.

Algee-Hewitt and Wheat's research indicated that some of the inter-landmark measurements of the digitizer and the laser scans were not statistically comparable (2). While this seems grim for the use of these different platforms, the authors were able to attribute this difference to variation between the samples that they used. The authors also found a statistically significant difference between the coordinate position of a few measurement landmarks (2). However, this information is outside of the scope of this research project since landmarks were not separated using a class system. However, this

information is considered in the discussion of the data since it is pertinent to the comparison of this research project to their research. In addition to three dimensional laser scanning, anthropologists also have the option to use photogrammetry as a means of 3-D model making. It is more difficult to conceptualize than 3-D laser scanning; however, the color of the models produced using 3-D photogrammetry are more accurate.

Photogrammetry

In its most basic form, photogrammetry is simply the measurement of photographs (16). 3-D photogrammetry is an expansion of this process, and involves taking multiple photographs of a single object from different angles. When the angle of the photograph is combined with the position of the camera, information about where the object lies in 3-D space can be determined, and this information can be used to create a 3-D object (23). There is a broad range of research that has been done using 3-D photogrammetry ranging from artifact curation to more forensic science related subjects such as blunt force trauma modeling and biological sex estimation (4, 6, 9, 16, 18, 19). Research that discusses the accuracy of the measurements taken using three-dimensional photogrammetry is very limited; however, best practices for obtaining high quality three dimensional models have been published (4, 12).

These best practices were implemented in the development of models created for this study. Outside of 3-D photogrammetry and 3-D laser scanning, anthropologists can use a 3-D Microscribe digitizer to create 3-D models.

Microscribe 3-D Digitizer

The three-dimensional Microscribe Digitizer is a piece of equipment that derives measurements from an object by plotting points in 3-D space in relation to the Microscribe unit. This means that the Microscribe is functioning as the origin in a coordinate system for all of the points that are taken. In this way, the 3-D digitizer is

different than the 3-D laser scanner or 3-D photogrammetry since there is a true 3-D model is not produced unless photographs are overlaid on the measurement points. After all of the points are recorded on the object, in this case a human skull, the distances between the points are calculated. This method has been shown to be accurate in the past through applications that utilized this technology to estimate ancestry and others that directly assessed the accuracy of the of the Microscribe (22). Studies have previously shown that the Microscribe has a standard deviation of only .12 millimeters (mm), meaning that this technology is equivalent to or less variable than hand derived measurements of the skull (22).

Within the field of anthropology, most research that has been done on 3-D image capturing has focused on the ability to curate large collections (3, 6, 8, 10, 14, 21). This means that there has been very little research on the comparability of these technologies and how variable measurements are on a single platform (2, 7, 20). This project sought to address this issue by comparing measurement data collected using different virtual methods: 3-D photogrammetry, a MicroScribe 3-D Digitizer, and 3-D Laser Scanning. A systematic comparison of these technologies with traditional metrics provides greater knowledge about the evolving technology of 3-D artifact curation. It will ensure that future research done using these technologies considers their variability, and it will ensure that researchers who perform data collection on 3-D models know the potential inaccuracies that could result. Further, since there is no methodology developed for the creation of 3-D models, the methodology presented here could serve as basis for future methods created for 3-D modeling of crania.

Materials and Methods

To evaluate the accuracy of the 3-D Laser Scanner, the 3-D MicroScribe digitizer, and 3-D Photogrammetry compared to hand held measurements, three datasets of all cranial measurements were recorded three time for each skull were, for an overall total of nine measurement sets. The averages and ranges for the datasets were then used to determine if there was a statistically-significant difference between each of the technologies when compared to traditional hand-held metrics. Additionally, the averages were compared across datasets for a single platform and skull to examine if there was a statistically significant difference between measurements taken on a single technological platform.

Two of the skulls were obtained from a biological supply company. The third skull was a cast from a biological supply company. These individuals will be referred to as Individual 1, Individual 2 (cast), and Individual 3. A description of each cranium used in this research can be seen in Table 1, and a visual representation of each cranium used in this study can be seen in Images 1 through 6. The cranial suture closure of the individuals was an important factor to consider since many of the landmarks used to make cranial measurements are located at the intersection of these sutures. Not being able to see these sutures could easily result in measurements being taking erroneously. Thus, this information was taken into consideration when the statistical analyses were interpreted since it could artificially affect the statistical significance of a technological platform. In interpretation, it could make it seem as if one dataset from a technology was less effective than another, despite the differences being due to the general shape and condition of the cranium.

Table 1: Description of each skull used in the analysis of craniometrics.

DESIGNATION	ANCESTRY	SUTURE DESCRIPTION	TAPHONOMIC DAMAGE
INDIVIDUAL 1	European	Sutures are very faint but still visible in some areas.	Post processing bleaching renders some of the sutures very difficult to see.
INDIVIDUAL 2 (CAST)	African	Sutures are nearly obliterated, and very few are easy to see.	No taphonomic damage present.
INDIVIDUAL 3	European	Sutures are clearly defined and easy to identify across the whole cranium.	There is slight damage present to the left maxilla near prosthion.

Measurements of the models generated from these individuals were then made according to the guidelines put forth in the *Data Collection Procedures for Forensic Skeletal Material* (13). These measurements were then compared across each technique: 3-D Laser Scanner, 3-D MicroScribe, and 3-D Photogrammetry.



Figure 1: Photograph of the anterior view of Individual 2 Cast



Figure 2: Photograph of the superior view of Individual 2 cast's skull illustrating the degree of cranial suture fusion.



Figure 3: Photograph of the anterior view of Individual 3 note the slight taphonomic damage to the maxilla, superior to the central incisors.



Figure 4: Photograph of the superior view of Individual 3's Skull Illustrating the Degree of cranial suture closure.



Figure 5: Photograph of the anterior view of Individual 1



Figure 6: Photograph of the superior view of Individual 1's skull illustrating the degree of cranial suture closure.

Hand Held Metrics

For each skull, hand-held metrics were performed to serve as a control for the other measurement styles. These measurements were taken according to the guidelines in the *Data Collection Procedures for Forensic Skeletal Material* (13). A subset of the measurement landmarks used in this project can be seen in Figure 7. For a more exhaustive list refer to the Index. The tools used to take these measurements were sliding calipers and spreading calipers, and the tool utilized for each measurement varied depending on the recommendations found in the manual. All of the measurements were then converted into millimeters (mm) to provide a consistent measurement unit for each technology.

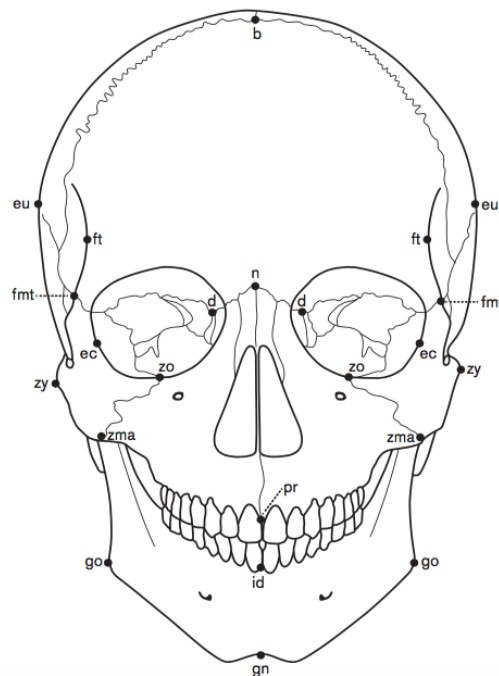


Figure 7: Diagram illustrating a subset of the cranial landmark measurements taken, from *Data Collection Procedures for Forensic Skeletal Material* (13).

3-D Scanner

To obtain a three-dimensional model using the NextEngine scanner (NextEngine, Inc. Santa Monica, CA, USA), each skull was placed on a platform that was rotated in twenty-degree increments until a full 360-degree scan was created. This process was then repeated with the skull resting on its external occipital protuberance with the maxilla facing superiorly in order to obtain the inferior and superior portions of the crania. Additional scans of the eye orbits were made in order to generate an image of the entire surface, since neither of the positions previously mentioned gave the scanner a complete view of the orbital surface. To create the final three-dimensional image, the individual scans from each twenty-degree rotation were manually aligned using cranial landmarks and features that were easily identifiable in each image.



Figure 8: Set-up used for the NextEngine 3-D Laser Scanner.

The models produced were then imported into Meshlab to be measured (5).

Meshlab is an open-source software designed for the creation and optimization of three-dimensional meshes or models (5). In order for the models to be measured within Meshlab, it was first necessary to scale them to reality. To do this, a physical measurement of the skull was taken, and this measurement was manually divided by the number produced in the computer program to create a ratio between reality and the 3-D model (5).

After the model was scaled to reality, the measurements for each skull were taken on the screen in a similar way to hand held metrics. Points were placed on each cranial landmark and the measurements produced by the software were recorded on the data sheet provided in the *Data Collection Procedures for Forensic Skeletal Material* (13). Unlike the Agisoft software utilized in three dimensional photogrammetry (discussed below), there is not a measurement that retains the scaling value. Therefore, there is no overly consistent value in the data.

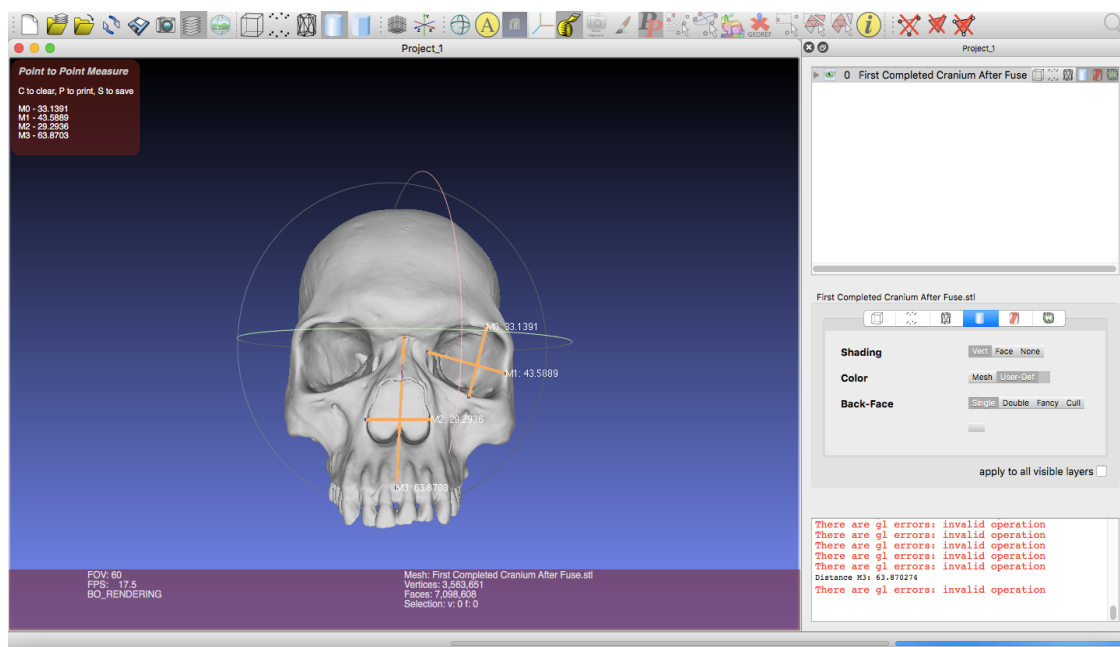


Figure 9: 3-D Model of Individual 2 generated by the NextEngine Laser Scanner illustrating a subset of measurement points placed in Meshlab.

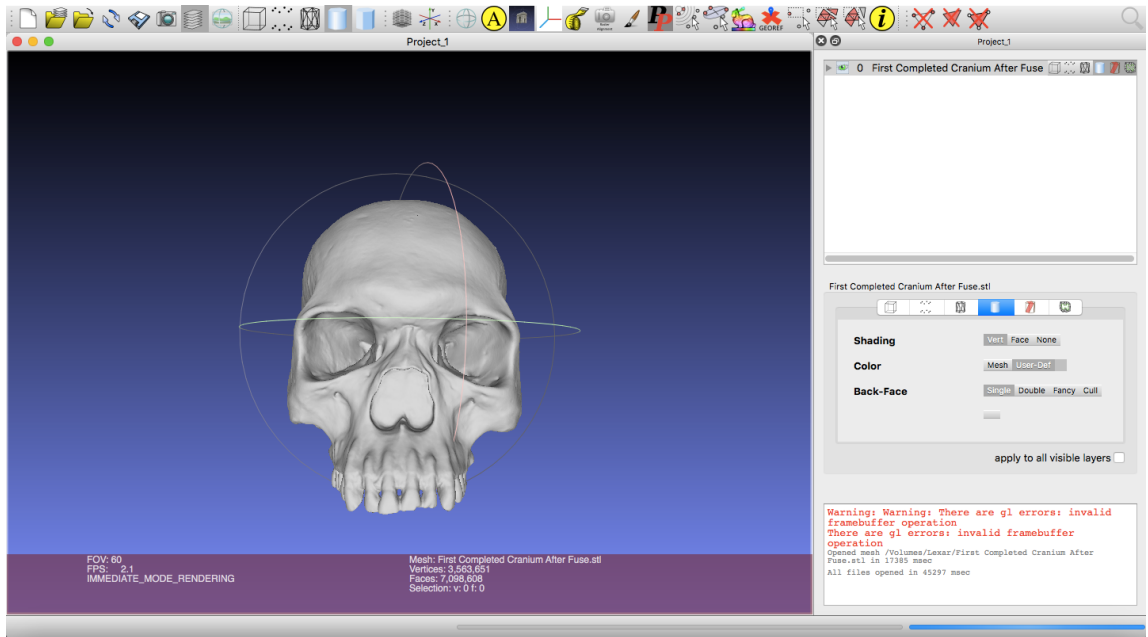


Figure 10: 3-D Model of Individual 2 created by the NextEngine Laser Scanner placed in Meshlab.

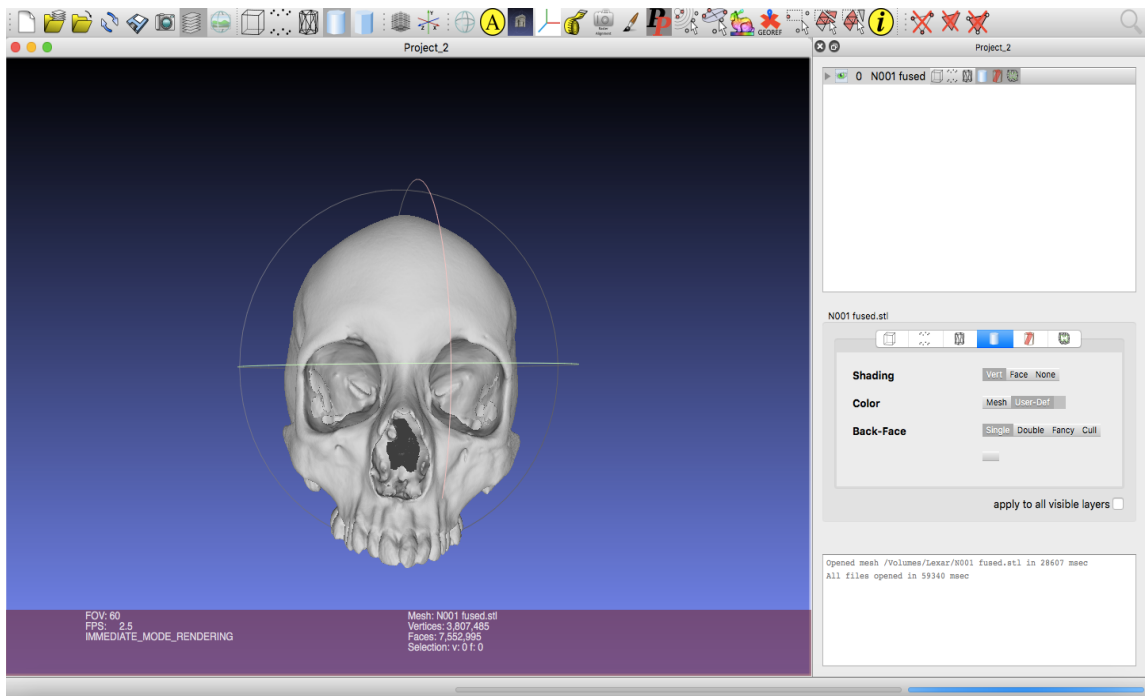


Figure 11: 3-D Model of Individual 1 created by the NextEngine 3-D Laser Scanner placed in Meshlab.

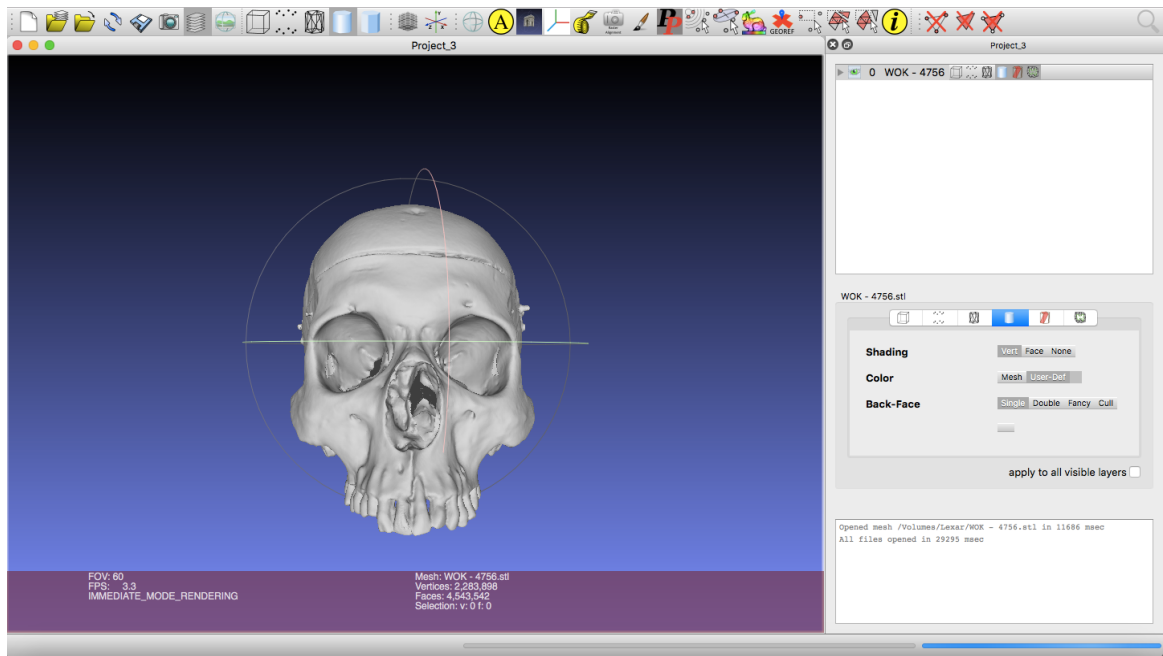


Figure 12: Model of Individual 3 created using the NextEngine 3-D Laser Scanner placed in Meshlab.

3-D Photogrammetry

The methodology to produce three-dimensional models using photogrammetry was slightly different than the methods used to create three-dimensional models with the NextEngine Scanner. To create a three-dimensional model using photogrammetry, a Nikon DSLR (model number) was set on a tripod approximately 1-2 feet from the skull. However, in order to get the skull into focus the camera had to be repositioned occasionally. The camera was fixed with a 50 mm lens and the aperture was set to f/16, a very small aperture, to allow for the greatest depth of field possible. Soft box lighting, a photobox and box lights were used in the photographs. A visual representation of this can be seen in figures 13 and 14. If the pictures of the skull were too dark, adjustments to the shutter speed of the camera were made to produce a brighter picture. The pictures that were too dark or too blurry to be used were removed from the camera roll to speed up the production of the three-dimensional model.

The skull was placed on a rotating platform with increments marked at every twenty degrees, and black velvet was hung behind this platform to make it easier to remove the background during image processing. A photograph was taken each time the skull was rotated twenty degrees. The same procedure that was used with the 3-D laser scanner was used here, in order to capture the base and the top of the skull. The skull was placed on its external occipital protuberance with the maxilla pointed superiorly. After obtaining these photos, close-up photos were taken of the eye orbits at various angles in order to capture the entire orbital surface.



Figure 13: Photogrammetry set up with Individual 2 placed on the rotating turn table. Softbox lights are set up above and to the right and left of the subject. Can lights are set in front of the subject beside the camera.



Figure 14: Position of camera relative to subject during shooting.

The photos taken of the crania were then imported into Metashape, a three dimensional software program designed by Agisoft LLC and released in 2018 (1). This software was chosen since it was optimized for the analysis of models created via photogrammetry. Once photographs were imported into Metashape, they were edited to remove background objects using the masking tool available in the software (1) (Agisoft LLC. v. 1.5 2018). This was done to speed up the processing time and create a models that needed post processing clean up. Once the photographs were edited they were aligned on the medium setting in within Metashape. If the photographs did not align properly, they were aligned based on markers manually placed at cranial landmarks. Once the models were created, any extraneous points picked up by the camera that were still in the models were removed in order to produce a more refined three dimensional model.

When the final model was produced, measurements were taken within Metashape by placing markers on the cranial landmarks since Metashape has an on board measuring system that can automatically render distances (1) (Agisoft LLC. v. 1.5 2018). A scale bar was then created between those markers, and after imputing a scaling measurement into the software, point-to-point measurements were taken. A subset of these measurements can be seen in Figure 15, and all other models can be seen in Figures 16-18. After this scaling measurement was placed in the software, other measurements were taken across the skull by generating additional scale bars between measurement points. These measurements were estimated based on the value manually input to scale the model. This scaling measurement was marked on each of the data sheets since it was more consistent than any of the other measurements which would skew any data analysis that was performed on this measurement.

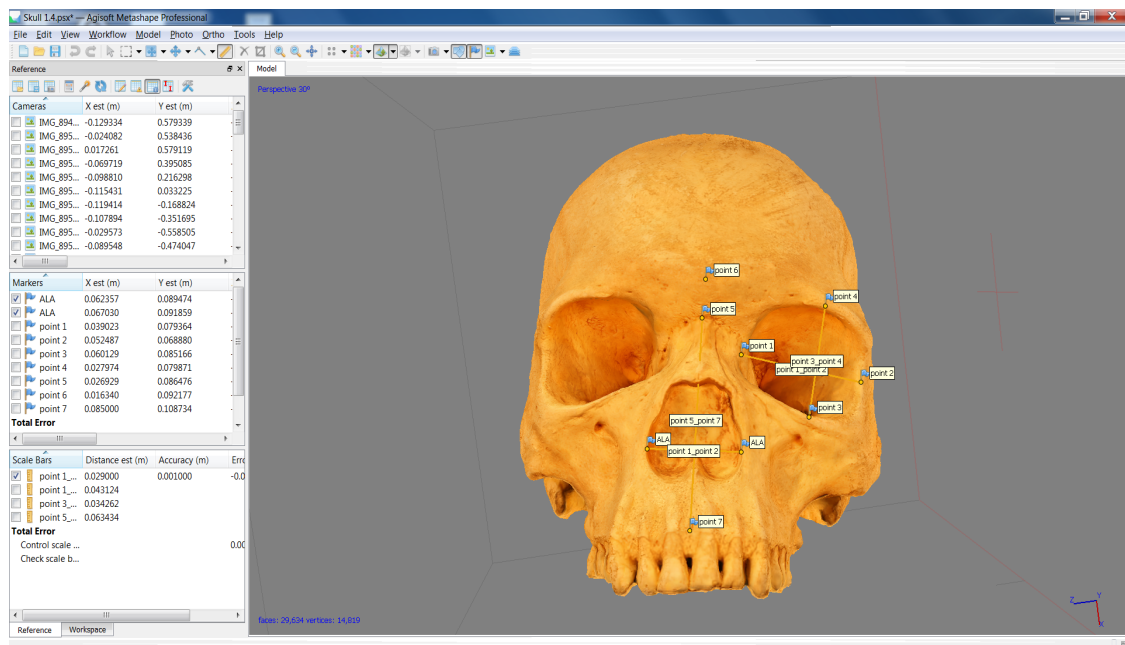


Figure 15: 3-D model of Individual 2 (cast) produced by photogrammetry with a subset of measurements placed across the skull.

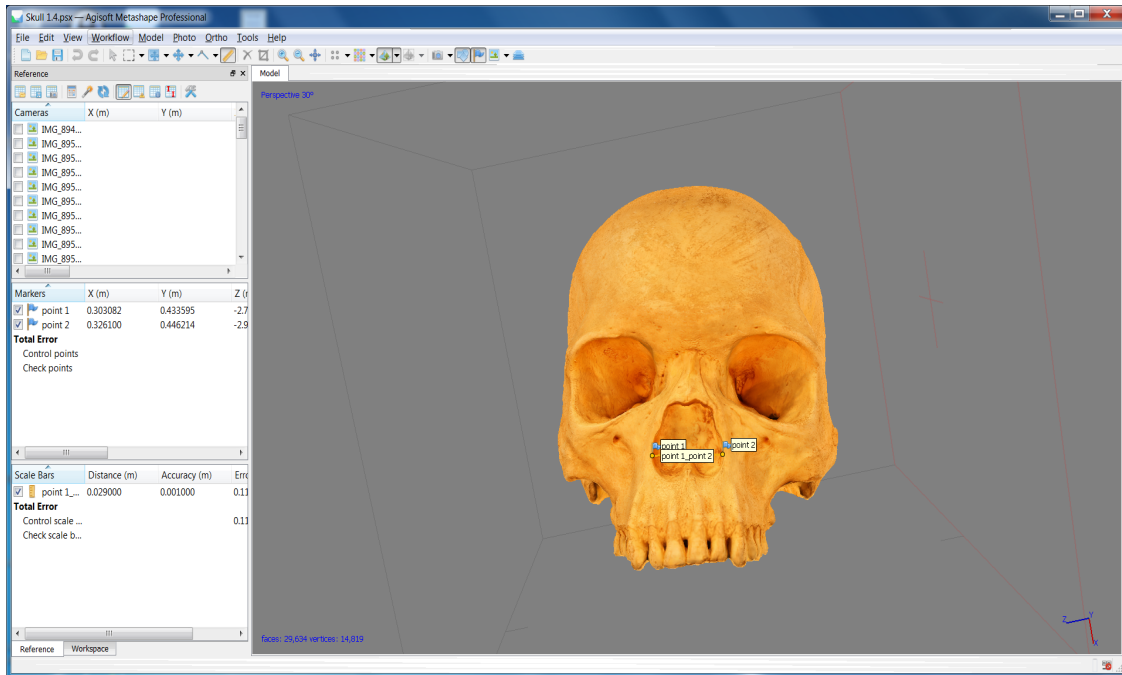


Figure 16: 3-D model of Individual 2 (cast) created via photogrammetry.

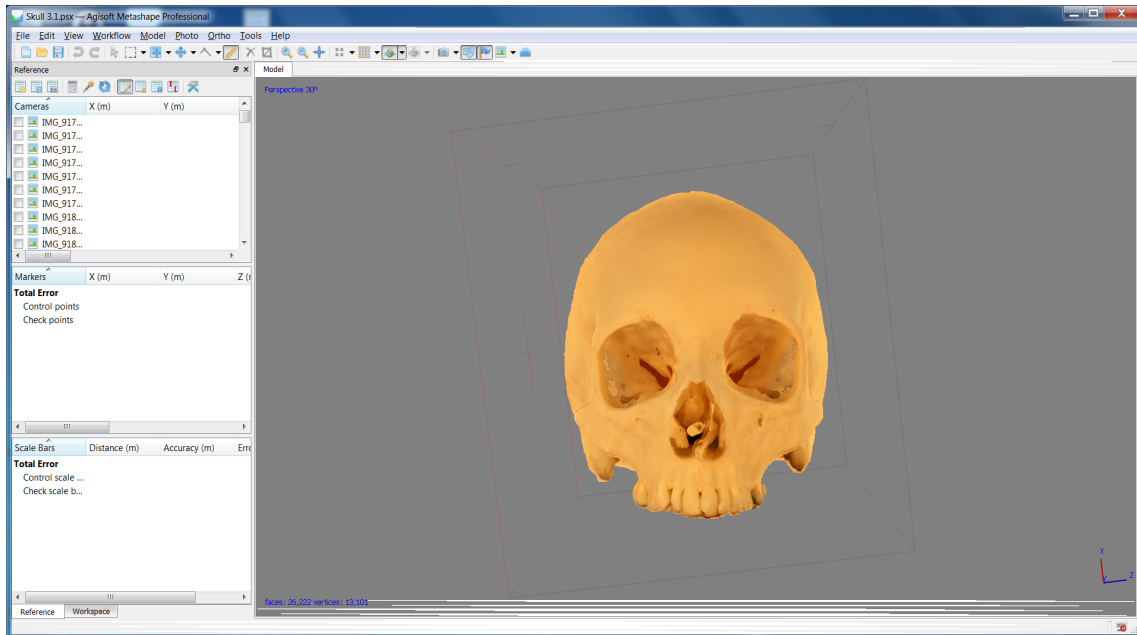


Figure 17: 3-D model of Individual 1 created via photogrammetry.

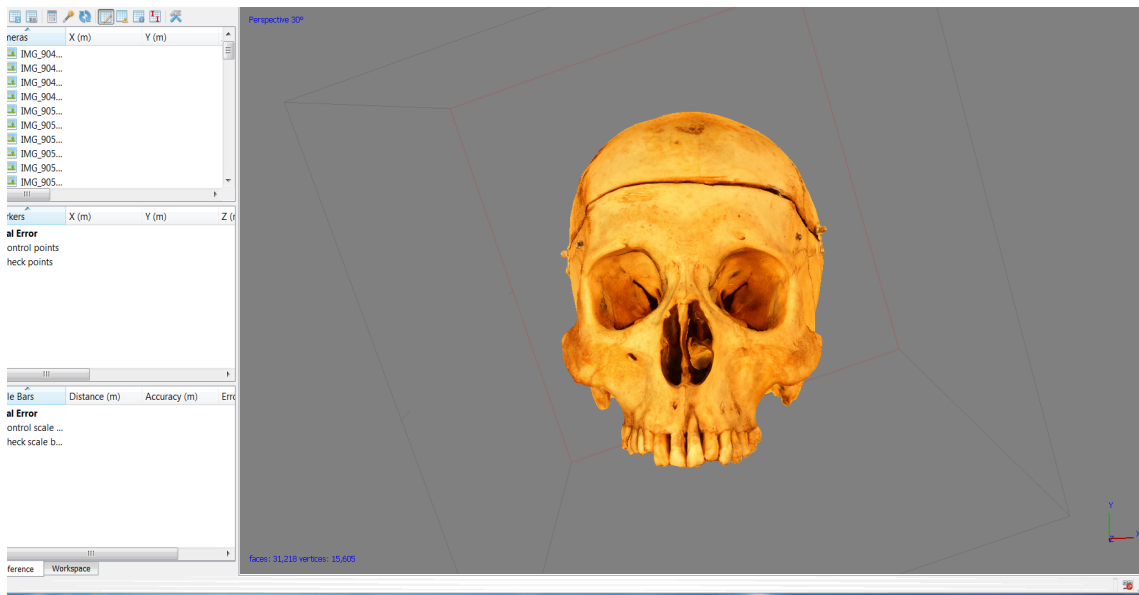


Figure 18: 3-D model of Individual 3 created via photogrammetry.

Microscribe Digitizer

The measurements for the Microscribe Digitizer were taken in the 3Skull software (15), and individual points were identified from definitions provided by the *Data Collection Procedures for Forensic Skeletal Material* (13). Unlike the other 3-D technologies used the Microscribe Digitizer does not automatically generate a 3-D model. It has the potential to be overlaid onto an image, but for this research only the points collected in 3-D space were used. The standard set-up for the Microscribe Digitizer was to position the skull on three clay pillars next to the Microscribe where all of the measurement points could be reached without moving the digitizer. This set up can be seen in Figure 19. If the digitizer did move, the process would have to be restarted since the digitizer unit bases all measurements off its original placement, and any movement from that area would reset the origin point for the data.

After each the cranial landmarks were recorded, the 3Skull software automatically generated all of the cranial measurements and placed them in a table. These measurements were derived based on the recorded location of the cranial landmarks and their distance from one another in three-dimensional space.



Figure 19: Typical set up of the Microscribe 3-D Digitizer.

Results

Each dataset was examined for obvious outliers, and these measurements were excluded from the analysis. In addition to outlying measurements, maximum alveolar length (MAL) and mastoid height (MDH) were excluded due to variations in the recording method during this research project. Exclusion of these measurements prevented further skewing of the results. Zygoorbitalic breadth (ZOB) was removed from analysis because it was not calculated by 3Skull software, making it impossible to

compare this measurement across all technological platforms. Additionally, there were two zero (0) values that were not captured by the 3Skull Software which were removed prior to the analysis.

The data were analyzed using two different statistical methods: Levine’s Equality of Variance and an Analysis of Variance (ANOVA) test. Levine’s Equality of Variance test was performed on the averages and the ranges between each technology to see if there was a statistically significant difference in the variances between the technological platforms. Additionally, the ranges from each technological platform were computed for each data set and these were compared between the platforms to see if there was a significant difference in the spread of the data between technologies. This would be further indication that landmarks could be reliably identified between technologies. For these tests a *p*-value of .05 was used to determine significance.

Table 2: Comparison of the Microscribe 3-D Digitizer to hand-held metrics for each dataset.

DATA SETS	SIG. VALUE	SKULL
1	.985	Individual 1
1	.904	Individual 2 (cast)
1	.981	Individual 3
2	.818	Individual 1
2	.885	Individual 2 (cast)
2	1.0	Individual 3
3	.972	Individual 1
3	.912	Individual 2 (cast)
3	.952	Individual 3

Table 3: Comparison of the NextEngine 3-D Laser Scanner to hand-held metrics for each data set.

DATA SET	SIG. VALUE	SKULL
1	.992	Individual 1
1	.945	Individual 2 (cast)
1	.963	Individual 3
2	.900	Individual 1
2	.999	Individual 2 (cast)
2	.971	Individual 3
3	.903	Individual 1
3	.943	Individual 2 (cast)
3	.947	Individual 3

Table 4: Comparison of 3-D photogrammetry to hand-held metrics for each data set.

DATA SET	SIG. VALUE	SKULL
1	.962	Individual 1
1	.979	Individual 2 (cast)
1	.958	Individual 3
2	.996	Individual 1
2	.947	Individual 2 (cast)
2	.966	Individual 3
3	.975	Individual 1
3	.827	Individual 2 (cast)
3	.922	Individual 3

In many of the tests seen between Tables 2 through 4, the *p-values* often exceeded .90, indicating there were no statistically-significant differences found between the averages of the measurements taken on the three dimensional models to the measurements taken by hand. This indicates that there is very little variance between measurements taken by hand on a physical skull and measurements taken by selecting points across the surface of a three dimensional model.

There were no statistically-significant differences found when comparing the averages of each dataset across a single technology either, and this can be seen in Tables 5 through 8. The *p*-values for this comparison were very similar to those derived by comparing the measurement platforms. They often exceeded .90, indicating very little variance between the averages of each dataset for a single measurement technology. This indicates that cranial measurement points were able to be reliably identified.

Table 5: Comparison of Measurement data sets for Hand Held metrics

DATA SET	SIG.	SKULL
1 V. 2	.982	Individual 1
1 V. 2	.998	Individual 2 (cast)
1 V. 2	.991	Individual 3
1V. 3	.990	Individual 1
1V. 3	.896	Individual 2 (cast)
1V. 3	.988	Individual 3
2 V. 3	.992	Individual 1
2 V. 3	.898	Individual 2 (cast)
2 V. 3	.979	Individual 3

Table 6: Comparison of Measurements between data sets for Measurements taken on Photogrammetry Models

DATA SET	SIG.	SKULL
1 V. 2	.948	Individual 1
1 V. 2	.971	Individual 2 (cast)
1 V. 2	.999	Individual 3
1V. 3	.977	Individual 1
1V. 3	.954	Individual 2 (cast)
1V. 3	.976	Individual 3
2 V. 3	.971	Individual 1
2 V. 3	.983	Individual 2 (cast)
2 V. 3	.975	Individual 3

Table 7: Comparison of Measurements between data sets for Measurements taken on Models produced by the NextEngine Laser Scanner.

DATA SET	SIG.	SKULL
1 V. 2	.925	Individual 1
1 V. 2	.947	Individual 2 (cast)
1 V. 2	.983	Individual 3
1V. 3	.919	Individual 1
1V. 3	.990	Individual 2 (cast)
1V. 3	.972	Individual 3
2 V. 3	.993	Individual 1
2 V. 3	.956	Individual 2 (cast)
2 V. 3	.954	Individual 3

Table 8: Comparison of Measurements between data sets for the Microscribe 3-D Digitizer.

DATA SET	SIG.	SKULL
1 V. 2	.784	Individual 1
1 V. 2	.981	Individual 2 (cast)
1 V. 2	.989	Individual 3
1V. 3	.998	Individual 1
1V. 3	.919	Individual 2 (cast)
1V. 3	.983	Individual 3
2 V. 3	.783	Individual 1
2 V. 3	.899	Individual 2 (cast)
2 V. 3	.972	Individual 3

The ANOVA test further supports these results, indicating that there is little difference between averages of the measurements for each dataset, and there is little difference between the averages of each technology. This can be seen in Figures 20 through 22 since more separated variables indicate that they are having a greater effect on the measurements. The only significant factor for this analysis was the skull that was used. Given that each of the crania used had different ancestries, this made sense because

each ancestry typically has a specific set of average measurements. This means that making a comparison between the crania would be difficult and likely to introduce statistical variation.

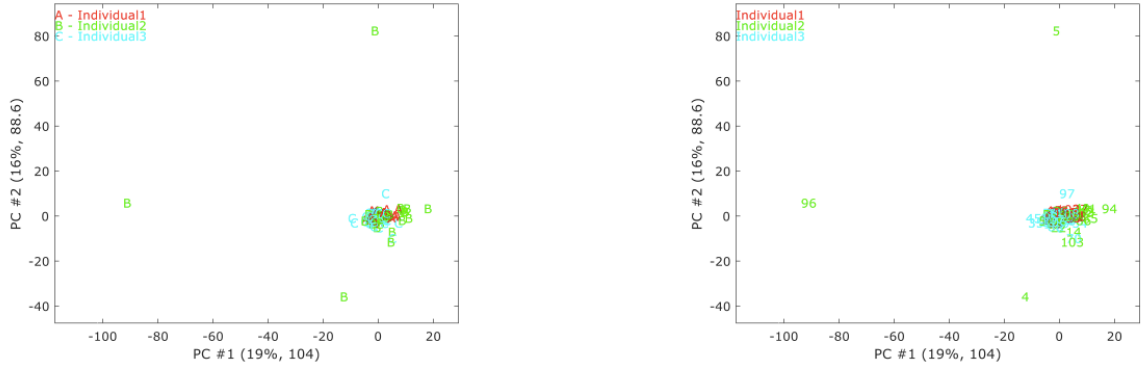


Figure 20: ANOVA graph illustrating the relatedness of different variables. In this case it is illustrating datasets.

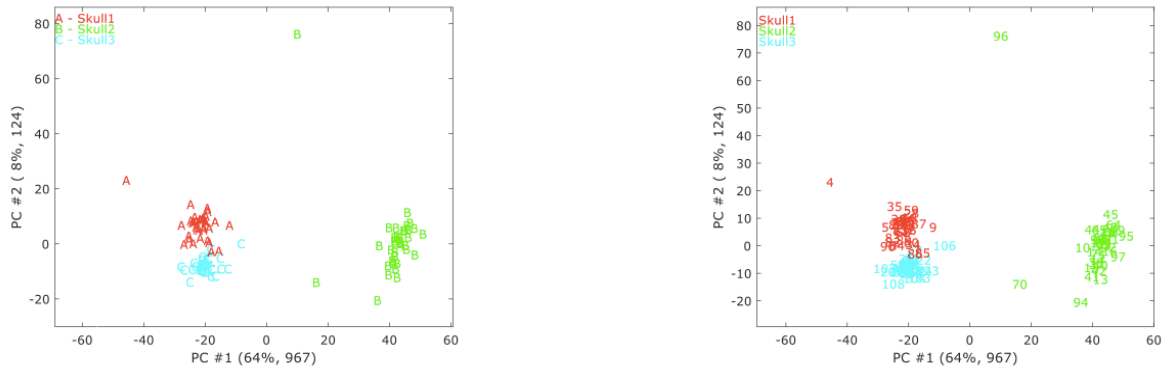


Figure 21: ANOVA graph illustrating the relationship of the Individual skull to the measurements.

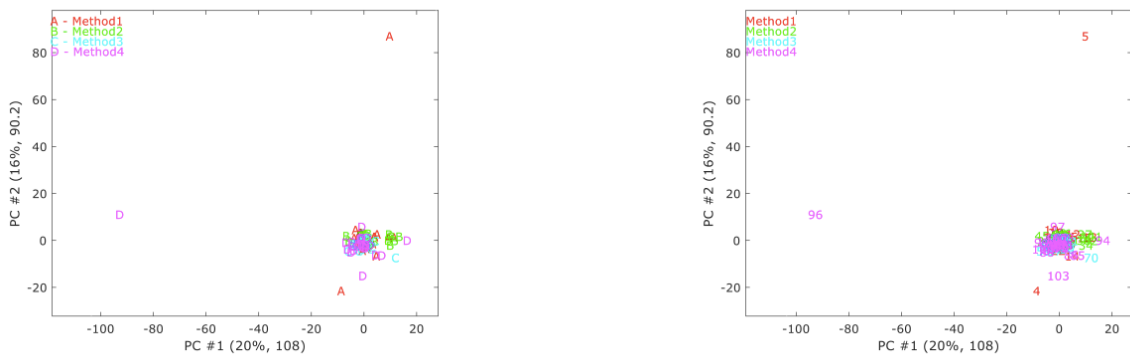


Figure 22: ANOVA graph illustrating the relationship of the technological platform to the measurements produced.

The tests presented in Tables 9 through 11 illustrate a comparison of the ranges of each of technological platform to the ranges of the hand held measurements. Nearly all of the tests returned values that were not statistically significant indicating that there is also no difference in the ranges of an observer between technological platforms. However, there were three values that fell below the p -value of .05 indicating that there was a significant difference between the ranges on a technological platform. These occurred between the digitizer and hand-held metrics, and they occurred between 3-D photogrammetry and hand-held metrics. All the differences except one were confined to two different skulls possibly indicating that physical differences in those skulls were the cause of the statistical variance.

Table 9: Comparison of the ranges of the measurements taken with the Microscribe 3-D digitizer to the ranges of measurements taken with Hand Held Instruments.

DATA SET	SIG	SKULL
1	.715	Individual 1
1	.924	Individual 2 Cast
1	.108	Individual 3
2	.634	Individual 1
2	.205	Individual 2 Cast
2	.129	Individual 3
3	.014	Individual 1
3	.080	Individual 2 Cast
3	.760	Individual 3

Table 10: Comparison of the ranges of measurements taken on Models made with the 3-D laser scanner to the ranges of measurements taken on Hand Held Instruments.

DATA SET	SIG	SKULL
1	.313	Individual 1
1	.711	Individual 2 Cast
1	.130	Individual 3
2	.130	Individual 1
2	.089	Individual 2 Cast
2	.546	Individual 3
3	.697	Individual 1
3	.139	Individual 2 Cast
3	.374	Individual 3

Table 11: Comparison of the ranges of measurements taken on Models made with the 3-D Photogrammetry to the ranges of measurements taken on Hand Held Instruments.

DATA SET	SIG	SKULL
1	.396	Individual 1
1	.411	Individual 2 Cast
1	.385	Individual 3
2	.099	Individual 1
2	.045	Individual 2 Cast
2	.427	Individual 3
3	.170	Individual 1
3	.401	Individual 2 Cast
3	.029	Individual 3

Discussion

The results of this project indicated that there is no statistically-significant difference between the averages of the measurements taken using the different technological platforms. This was consistent with Algee-Hewitt and Wheat's research (2)

which compared measurements taken from models made with a three-dimensional laser scanner to measurements taken with a digitizer. However, one of the interesting factors about Algee-Hewitt and Wheat's research is that they found Type III landmarks, which are instrumentally determined, to be more variable than Type I measurements, which are often found at the intersection of two bones, or Type II measurements which are found at the greatest curvature (2). While this research did not directly make any comparisons between landmark types, it is interesting to note that there did not seem to be any correlation to this variation within the overall measurement. It would be expected that there would be significant difference between some of the measurement platforms had there been the same variance that Algee-Hewitt and Wheat had noted. Additionally, the information found by Sholts et. al. in 2011 (20) indicated that Type II landmarks were often more variable than Type III landmarks. This could indicate that the differences found between the coordinate location of measurement points is slight enough to play only a small role in a complete measurement since previous research is yielded conflicting results, and this research indicates that there is no statistically-significant variation between measurements taken between platforms.

Another interesting outcome that occurred within Algee-Hewitt and Wheat's research was that two of the eight measurements that were taken yielded statistically-significant differences between the three-dimensional scanner and the digitizer (2). While there are many factors that could contribute to the differences between this research project and prior research, it could be that prior data were more variable since individualized scans were not used to complete the orbital surface or scans that would complete the inferior portion of the skull around the foramen magnum. This would affect the overall quality of the scan, and it could make a difference in the placement of landmark points.

This suggests that it is incredibly important to create precise models that capture as much of the object's surface as possible. There is currently no standardized process or best practices in place for how to create three-dimensional models of crania; however, when these documents are produced in the future, this factor should be taken into account. This may make the creation of a set protocol difficult to produce, since it necessitates variability in each set-up, since each skull is unique and presents its own challenges. However, capturing all the surfaces of the skull should be given priority over a hard rule governing the orientation of the skull.

Furthermore, it should be noted that one area of difficulty in this project came down to following a set method. Often times in the photogrammetric process it was necessary to slightly reposition the camera in order to get the entire cranium in focus. Additionally, the photographs of Individual 1 would not align in a way that produced a complete mesh. Since it was determined that obtaining all surfaces of the skull should take priority, the skull was rotated in ten degree increments instead of the traditional twenty degree increments that had been used previously. This slight change produced a satisfactory three-dimensional model. While it did result in a slight change in methodology, it did not change the accuracy of the measurements taken on this model showing that the model was still comparable to the other three-dimensional models.

While there was not a statistically-significant difference between the averages of the technological platforms when comparing each dataset, there was a statistically-significant difference between the ranges. This could indicate that there are greater degrees of variability in measurements for technologies such as the Microscribe 3-D digitizer and the 3-D photogrammetry since averages can flatten out variability that occurs within a dataset. But, it is important to consider some of the intrinsic factors of the skulls when interpreting this analysis. Of the individual skulls analyzed, two of the three

that returned statistically-significant results were Individual 1 and Individual 2 (cast). Both of these individuals had a high degree of cranial suture closure making several landmarks such as bregma, zygomaxillare, and lambda difficult to identify. This could contribute to a greater degree of variability and spread within the data set which would lead to there being a statistically significant difference between the ranges.

Another cause of this statistical variation could be the size of the sample. Since the range was calculated across only three measurement sets, outliers may be more difficult to spot, and may have a greater effect on data comparison. This could lead to skewed results, and in future analyses, a larger sample size should be considered since it would make the data less variable and it would allow for a comparison of standard deviations. This would allow for a better comparison between individual measurements since it would be evaluating how far the data are spread from the mean not just entire spread of the data for a measurement. In this way, the standard deviations would give a more nuanced description of the data.

To see if there was an interpretative difference between the craniometrics taken between the technological platform, the average measurements of each dataset for Individual 2 cast were input into FORDISC 3.0 (15) a software program designed by Richard Jantz and Doug Owsley to determine ancestral probability. The program performs a multivariate discriminant function analysis on craniometrics to assess the likelihood that an individual is a specific ancestry. It has fairly large sample sizes and can be updated by anthropologists who choose to submit populations into the software.

After inputting one measurement set for Individual 2 (cast), FORDISC reported an African ancestry male. This report stayed consistent across all data sets for each technology. This shows that FORDISC was able to consistently interpret the craniometrics of Individual 2 (cast) across technological platforms, and it is important to

consider this interpretive difference especially within forensic anthropology since ancestry is a key part of a biological profile. Additionally, if future researchers were to use this technology to curate skeletal material from case work it would be essential to ensure that each technology created models that produced interpretively similar results.

Conclusion

This study demonstrated that there is no statistically-significant difference between average measurements taken on models created via three-dimensional laser scanner, three-dimensional photogrammetry, Microscribe digitizer, and traditionally derived measurements. While there were statistically significant differences between the ranges of some of the technological platforms, it is likely that these differences are due to intrinsic properties of the skull such as cranial suture closure and visibility of measurement land marks. More research could be done on this project with greater sample sizes to ensure that each of the technologies compares to hand held measurements. However, the majority of the analyses ran in this research indicated that there is no statistically-significant difference between the measurements collected from 3-D models created by the NextEngine laser scanner or the models created through 3-D photogrammetry when compared to hand held measurements, and there is no statistically-significant difference between the point-to-point measurements collected with the Microscribe 3-D digitizer and the measurements collected through hand-held instruments.

The results of this study support the use of these technologies as a form of digital curation that can be used to share three-dimensional models between researchers. In the future, these technologies could aid in research by giving greater access to skeletal collections. Additionally, within the criminal justice system, these technologies could

change the way that evidence is introduced in court and curated. This research provides a basis that could be expanded upon in the future since it validates the use of these technologies.

Works Cited

1. Agisoft Metashape software: agisoft.com January 1, 2019.
2. Algee-Hewitt, Bridget F.B, Wheat A. The Reality of Virtual Anthropology: Comparing Digitizer and Laser Scan Data Collection Methods for the Quantitative Assessment of the Cranium: Digitizer and Laser Scan Data Collection Methods. *American Journal of Physical Anthropology* 2016;160(1):148-155.
3. Bruno F. et. al. From 3-D reconstruction to virtual reality: A complete methodology for digital archaeological exhibition. *Journal of Cultural Heritage* 2010;(1):42-49.
4. Carlton C, Mitchell S, Lewis P. Preliminary Application of Structure from Motion and GIS to Document Decomposition and Taphonomic Processes. *Forensic Science International* 2018; 282 (41-45).
5. Cignoni P et. al. MeshLab: An Open-Source Mesh Processing Tool. Sixth Eurographics Italian Chapter Conference. 2008 (129-136).
6. Edward J, Rogers T. The Accuracy and Applicability of 3-D Modeling and Printing Blunt Force Cranial Injuries. *Journal of Forensic Sciences* 2018; 63 (683-691).
7. Errickson D et. al. Towards a Best Practice for the Use of Active Non-Contact Surface Scanning to Record Human Skeletal Remains from Archaeological Contexts: Active Non-contact Surface Scanning of Human Skeletal Remains. *International Journal of Osteoarchaeology* 2017;27(4):650-661.

8. Friess M. Scratching the Surface? The use of surface scanning in physical and paleoanthropology. *Journal of Anthropological Sciences* 2012;(90):1-26.
9. Guyomarc'h P et. al. New Data on the Paleobiology of the Gravettian Individual L2A from Cussac Cave through a Virtual Approach. *Journal of Anthropological Science* 2017; 14 (365-373).
10. Grosman L, Smikt O, Smilansky U. On the application of 3-D scanning technology for the documentation and typology of lithic artifacts. *Journal of Archaeological Science* 2008;35(12):3101-3110.
11. Jantz R. Ousley S. *FORDISC 3.1 Personal Forensic Discriminate Functions* 2005.
12. Katz D, Friess M. Technical Note: 3-D From Standard Digital Photography of Human Crania – A Preliminary Assessment. *American Journal of Physical Anthropology* 2014; 154 (152-158).
13. Langley N, Jantz L, Ousley S, Jantz R, Milner G. *Data Collection Procedures for Forensic Skeletal Material*. Knoxville, TN: University of Tennessee Knoxville, 2016
14. Means B, McCuiston A, Bowles C. Virtual Artifact Curation of the Historical Past and the NextEngine Desktop 3-D Scanner. *Technical Briefs in Historical Archaeology* 2013;(6):1-12.
15. Ousley SD. *Threeskull*. Version 2.0. 2010.
16. Papworth H, Ford A, Welham K, Thackray D. Assessing 3-D Metric Data of Digital Surface Models for Extracting Archaeological Data from Archive Stereoaerial Photographs 2016; 72 (85-104).

17. Photogrammetry. 2011. In Merriam-Webster.com. February 21, 2019 from meriam-webster.com/dictionary/photogrammetry.
18. Porter S, Huber N, Hoyer C, Floss H. Portable and Low-cost Solutions to the Imaging of Paleolithic Art Objects: A comparison of Photogrammetry and Reflectance Transformation Imaging 2016; 10 (859-863).
19. Sansoni G, et. al. Feasibility of Contactless 3-D Optical Measurement for the Analysis of Soft Tissue Lesions: New Technologies and Perspectives in Forensic Sciences. *Journal of Forensic Sciences* 2009; 54 (540-545).
20. Sholts S.B., Flores L, Walker P.L., Wärmländer S.K.T.S. Comparison of Coordinate Measurement Precision of Different Landmark Types on Human Crania Using a 3-D Digitiser: Implications for Applications of Digital Morphometrics. *International Journal of Osteoarchaeology* 2011; 21(535-543).
21. Shott M. Digitizing archaeology: a subtle revolution in analysis. *World Archaeology* 2014;46(1):1-9.
22. Stephen A, Wegscheider P, Nelson A, Dicky J. Quantifying the Precision and Accuracy of the Microscribe G2X Three-Dimensional Digitizer. *Digital Applications in Archaeology and Cultural Heritage* 2015; 2 (28-33).
23. Tucci G, Cini D, Nobile A. Effective 3-D Digitization of Archaeological Artifacts for Interactive Virtual Museum. *ISPRS - International Archives of the Photogrammetry, Remote Sensing and Spatial Information Sciences* 2012;35:413-420

24. Yilmaz M, Yakar M, Yildiz F. Digital Photogrammetry in Obtaining of 3-D Model Data of Irregular Small Objects. The International Archives of the Photogrammetry, Remote Sensing and Spatial Information Sciences. 2008; 37 (125-130).
25. <http://humanorigins.si.edu/evidence/3d-collection> (accessed 1-16-19).
26. <http://www.digitiseddiseases.org/mrn.php?mrn=R1007> (accessed 1-17-19)

Appendix

Used Measurement Landmarks According to the *Data Collections*

Procedures for Forensic Skeletal Material (13).

1. Alveolon – The point where the mid-sagittal plane of the palate is intersected by a line connection the posterior borders of the alveolar crests.
2. Asterion – The point where the temporal, parietal, and occipital bones meet.
3. Basion – The point at which the anterior border of the foramen magnum is intersected by the mid-sagittal plane opposite nasion.
4. Bregma – The posterior border of the frontal bone in the midsagittal plane usually at the meeting point of the coronal and sagittal sutures on the frontal bone.
5. Condylion – The most lateral points of the mandibular condyles.
6. Dacryon – Where the frontal, lacrimal, and maxillary sutures meet.
7. Ectoconchion – The intersection of the most anterior edge of the lateral orbital border and the line parallel to the superior orbital border that bisects the orbit into two equal halves.
8. Ectomolare – The most lateral point on the buccal surface of the alveolar margin.
9. Euryon – The most laterally positioned point on the side of the braincase.
10. Frontomolare Temporale – The most laterally positioned point on the frontomalar suture.
11. Frontotemporale – A point located generally forward and inward on the superior temporal line directly above the zygomatic process on the frontal bone.

12. Glabella – The most anteriorly projecting point in the mid-sagittal plane at the lower margin of the frontal bone which lies above the nasal root and between the superciliary arches.
13. Lambda – The apex of the occipital bone at its junction with the parietals in the midline.
14. Mastoidale – The most inferior point on the tip of the mastoid process.
15. Nasion – The point of intersection of the naso-frontal suture and the mid-sagittal plane.
16. Opisthocranium – The most distant point posteriorly from glabella on the occipital bone located in the mid-sagittal plane.
17. Opisthion – The point on the inner border of the posterior margin of the foramen magnum in the mid-sagittal plane.
18. Porion – The most anterior point along the upper margin of the external acoustic meatus.
19. Prosthion – The most anterior point on the alveolar border of the maxilla between the central incisors in the mid-sagittal plane
20. Radiculare – The point on the lateral aspect of the root of the zygomatic process at the deepest incurvature.
21. Zygion – The most laterally positioned point on the zygomatic arches.
22. Zygomaxillare Anterior – The intersection of the zygomaxillary suture and the limit of the attachment of the masseter muscle on the facial surface.
23. Zygoorbitale – The intersection of the orbital margin and the zygomaxillary suture.

Definitions of Used Measurements According to the *Data Collections Procedures for Forensic Skeletal Material* (13).

- 1.) Maximum Cranial Length – The straight-line distance from glabella to opisthocranium in the mid-sagittal plane.
- 2.) Nasio-Occipital Length – Maximum length in the mid-sagittal plane measured from nasion.
- 3.) Maximum Cranial Breadth – The maximum width of the skull perpendicular to the mid-sagittal plane wherever it is located with the exception of the inferior temporal line and the immediate area surrounding the latter.
- 4.) Bizygomatic Breadth – The maximum breadth across the zygomatic arches wherever found, perpendicular to the mid-sagittal plane.
- 5.) Basion - Bregma Height – The distance from basion to bregma
- 6.) Cranial Base Length – The distance from nasion to basion.
- 7.) Basion Prosthion Length – The distance from basion to prosthion.
- 8.) Maxillo-Alveolar Breadth – The maximum breadth across the alveolar borders of the maxilla measured on the lateral surfaces at the location of the second maxillary molars.
- 9.) Biauricular Breadth – The least exterior breadth across the root of the zygomatics.
- 10.) Nasion Prosthion Height – The distance from nasion to prosthion.
- 11.) Minimum Frontal Breadth – The distance between the right and left frontotemporale.
- 12.) Upper Facial Breadth – the distance between the right and left frontotmalare temporale.

- 13.) Nasal Height – The average height from nasion to the lowest point on the border of the nasal aperture on either side.
- 14.) Nasal Breadth – The maximum breadth of the nasal aperture.
- 15.) Orbital Breadth – The distance from dacryon to ectoconchion.
- 16.) Orbital Height – The distance between the superior and inferior orbital margins perpendicular to orbital breadth bisection the orbit into equal medial and lateral halves.
- 17.) Biorbital Breadth – The distance from left to right ectoconchion.
- 18.) Interorbital Breadth – The distance between right and left dacryon.
- 19.) Frontal Chord – The distance from nasion to bregma taken in the mid-sagittal plane.
- 20.) Parietal Chord – The distance from bregma to lambda taken in the midsagittal plane.
- 21.) Occipital Chord – The distance from lambda to opisthion take in the mid-sagittal plane.
- 22.) Foramen Magnum Length – The mid-sagittal distance from the most anterior point on the foramen magnum margin to opisthion.
- 23.) Foramen Magnum Breadth – The distance between the lateral margins of the foramen magnum at the point of greatest lateral curvature.
- 24.) Biasterionic Breadth – Straight-line distance from left to right asterion.
- 25.) Bimaxillary Breadth – The breadth across the maxillae from the left to the right zygomaxillare anterior.

